ARTICLE

C–H···S Hydrogen Bonding Interactions

Hazel A. Fargher,† Tobias J. Sherbow,† Michael M. Haley,* Darren W. Johnson,* and Michael D. Pluth*

Received 00th January 20xx,
Accepted 00th January 20xx

DOI: 10.1039/x0xx00000x

The short C–H···S contacts found in available structural data for both small molecules and larger biomolecular systems suggest that such contacts are an often overlooked yet important stabilizing interaction. Moreover, many of these short C–H···S contacts meet the definition of a hydrogen bonding interaction. Using available structural data from the Cambridge Structural Database (CSD), as well as selected examples from the literature in which important C–H···S contacts may have been overlooked, we highlight the generality of C–H···S hydrogen bonding as an important stabilizing interaction. To uncover and establish the generality of these interactions, we compare C–H···S contacts with other traditional hydrogen bond donors and acceptors as well as investigate how oxidation state, coordination number, and metal bonding affect the preferred geometry of interactions in the solid state. This work establishes that the C–H···S bond meets the definition of a hydrogen bond and serves as a guide to identify C–H···S hydrogen bonds in diverse systems.

Introduction

The past century has provided significant advances in understanding chemical bonding. Works such as "The Nature of the Chemical Bond" from Linus Pauling have detailed covalency through valence bond theory.[1] More broadly, we understand that non-covalent interactions play crucial roles in both small molecule and macromolecular structure, ranging from the impact of hydrogen bonding and π-stacking interactions in DNA to the London dispersion forces that stabilize sterically crowded inorganic and organometallic compounds.[2] While we continue to learn about these phenomena and their effects on contemporary chemical systems, we also understand that additional non-covalent interactions have been historically overlooked and are just now being realized for their potential.[3-5]

Hydrogen bonding (HB) interactions are among the strongest, most directional, and most dynamic of the many reversible, weak, primarily non-covalent interactions. These are especially important interactions because without HB, terrestrial life would not exist. For example, HB is responsible for the increased density of frozen water, the folding of proteins, and the self-complementarity of nucleic acids. A HB must feature both an attractive interaction and evidence of bond formation between a hydrogen atom bonded to a donor (D), which is more electronegative than the hydrogen, and an HB acceptor (A) with a lone pair of electrons.[6-8] Parameters that are often measured in HB systems include the H···A (L1) and D···A (L2) distances, and the D–H···A (A1) and R–A···H (A2) bond angles. Generally, shorter L1 distances and A2 angles approaching 180° contribute to stronger HB interactions (Fig. 1).

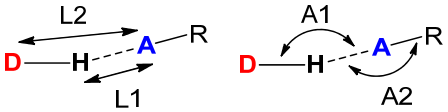

Fig. 1. Bond lengths and bond angles often measured in HB systems and will be described throughout the text.

Hydrogen bonding interactions are derived from a mixture of attractive and repulsive forces that include electrostatics, polarization, charge transfer, dispersion, and exchange repulsion.[8] Electrostatic forces are typically the largest contributing force in a HB and are directional based on the electrostatic potential of the D–H and A atoms. Electrostatic interactions can be enhanced by increasing partial charges on the donor and acceptor atoms, and therefore can be easily modified through functionalization. Of all the attractive forces, electrostatic interactions are the least dependent on interatomic distances, and therefore, the strength of these forces diminishes the least with increasing H···A distances. Polarization relates to the ability of the HB acceptor to reorganize electron density to better participate in hydrogen bonding. Charge transfer forces are caused by the overlap of a filled lone pair orbital on the HB Acceptor with the empty D–H antibonding orbital. These forces require high linearity and diminish greatly with deviation from optimal HB geometry and with increasing distance. Finally, dispersion and exchange repulsion forces are often referred together as van der Waals forces, which when combined can be approximated by the Lennard-Jones potential.[9] These forces are isotropic and

[a] *Department of Chemistry and Biochemistry, Materials Science Institute, Knight Campus for Accelerating Scientific Impact, and Institute of Molecular Biology, University of Oregon, Eugene, Oregon, 97403-1253, United States. haley@uoregon.edu, dwj@uoregon.edu, pluth@uoregon.edu*
† *These authors contributed equally to this work.*
Electronic Supplementary Information (ESI) available: CSD search parameters and methods, additional 3D histograms. See DOI: 10.1039/x0xx00000x

generally weak, which often makes them primary contributors to non-linear hydrogen bonds.

C–H Hydrogen Bond Donors

Studies surrounding the large field of hydrogen bonding are generally focused on traditional, strong hydrogen bonds, which are typically found between a highly electronegative HB donor, such as oxygen or nitrogen, and an electronegative HB acceptor. These strong interactions tend to be short and highly linear, with the D–H···A bond angle between 170 and 180°. The strength of these HB is generally measured by the distance between the hydrogen and acceptor atom in the solid state; however, spectroscopic techniques, such as ^{1}H NMR and vibrational spectroscopies, can also be used to characterize hydrogen bonds. With this emphasis on strong hydrogen bonds, weaker HB—which rely on a mixture of electrostatic, polarization, and van der Waals forces—have historically been overlooked. For example, despite the moderate electronegativity of carbon, C–H motifs have emerged as a newly recognized class of HB donors.[10-16] Early pK_a measurements of substituted benzoic acids showed an increased acidity of *ortho*-toluic acid in comparison to the *para* structural isomer, which was postulated to be due to a C–H···O intramolecular interaction between the methyl group and the carboxylate to stabilize the conjugate base (Fig. 2).[17] With many additional examples of C–H···O HB interactions demonstrated since this initial observation, including extensive theoretical calculations, it is now widely accepted that C–H···O interactions can be classified as HBs.[18] This classification has been expanded to include C–H···O, C–H···N, C–H···Cl, and C–H···Br HB interactions and has been well established in molecular biology,[19] organocatalysis,[20, 21] and molecular recognition.[22, 23] In fact, recent studies indicate C–H HB acidities follow predictable linear free energy relationships (LFER) and show modest isotope effects.[24, 25]

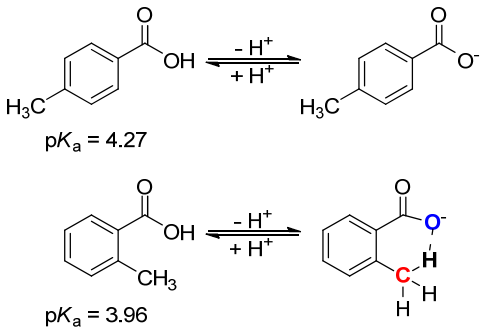

Fig. 2. Absence and presence of C–H HB in *p*-toluic acid and *o*-toluic acid, respectively.

C–H···S Hydrogen Bonding

Simply moving one row down the periodic table, however, we find that C–H···S HB interactions are underappreciated. Studies of S-based HB acceptors generally focus on N–H, O–H, and other more traditional HB donors, with little investigation of C–H···S HBs.[26-29] We find this omission surprising, as both work from our labs and others has shown that C–H HB donors exhibit a specific preference for sulfur-based HB acceptors.[30-33] For example, in our work in supramolecular anion recognition, we were inspired to investigate C–H HB donors for binding hydrosulfide (HS^-) after successful use of these receptors for Cl^- binding.[34] In 2016 we published an archetypal example of a supramolecular receptor for HS^-. Using ^{1}H NMR spectroscopy titrations and single crystal X-ray diffraction structural analysis of the host-guest complex, we showed that an aryl C–H functional group in the binding pocket participated in hydrogen bonding with HS^- and Cl^- (Fig. 3a,b) and even HSe^- (Fig. 3c).[31] Interestingly, the pyridine-based receptor, which could accept a S–H···:N(pyr) hydrogen bond from HS^-, resulted in weaker binding (~0.9 kcal/mol) than the benzene-based receptor with a C–H HB donor. Expanding on this preference for C–H HB donors, in 2019 we found that even when the aryl C–H bond was depolarized by an electron-donating *t*-Bu functional group, it still participated in hydrogen bonding with HS^-, HSe^-, Cl^-, and Br^-. This finding inspired a subsequent LFER investigation, in which we studied how modulating the polarity of the aryl C–H HB donor affected the anion-binding strength of HS^-, HSe^-, Cl^-, and Br^-. We found that these hosts displayed a preference for HS^- over the other three anions, in which increased binding strength was observed with increasing polarization of the C–H HB donor. In fact, HS^- was significantly more sensitive towards changing C–H HB donor polarity than the other three anions, which suggests a distinct sensitivity to C–H hydrogen bonding to the sulfur-containing guest. Furthermore, calculations indicated C–H···S HB strengths between 1-3 kcal/mol, which were more than double of those calculated for the C–H···Cl^- HB analogues. The only other two supramolecular hosts for HS^-, both published in 2018,[32, 33] also use C–H HB donors (Fig. 4) in the anion binding pocket, which further supports the idea that polarized C–H HB donors may be particularly important in HS^- recognition.

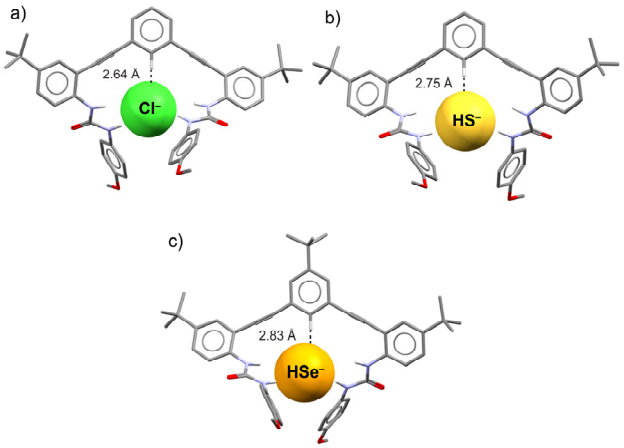

Fig. 3. Crystal structures of arylethynyl bisurea receptors shown to bind (a) Cl^-, (b) HS^-, and (c) HSe^- in the solid state. All three anions interact with the aryl C–H HB donor on the central ring.

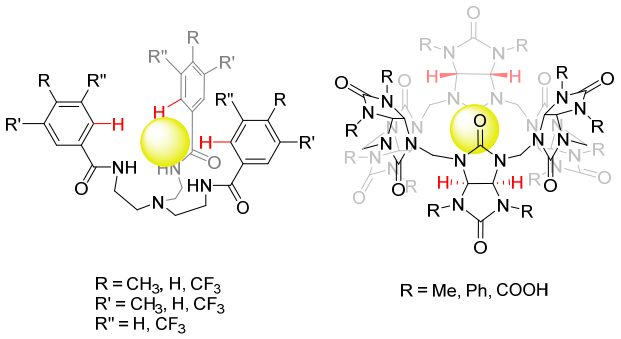

Fig. 4. Other supramolecular hosts demonstrated to reversibly bind HS^-. Both hosts feature C–H HB donors in their design (highlighted in red) and exhibit 1:1 binding with HS^- (depicted as a yellow sphere). Crystallographic structural data for these host-guest complexes have not been reported.

Recent work from our laboratory has also studied how reactive sulfur species (RSS) interact with metal-sulfur containing bonds, which led to the further isolation of compounds containing short C–H···S stabilizing contacts. For example, reaction of the molybdenum tetrasulfido complex $[NBu_4][TpMoS(S_4)]$ (Tp = hydrotris(3,5-dimethylpyrazol-1-yl)borate) with HS^- results in HS^- oxidation to form polysulfides and concomitant formation of a *tris*(sulfido) Mo complex $[NBu_4][TpMoS_3]$ byproduct.[35] Upon further inspection of the molecular structure of $[NBu_4][TpMoS_3]$, we found that the Mo=S bond lengths vary by up to 0.019 Å and that the longest Mo=S moieties displayed C–H···S contacts as short as 2.681 Å to the $[NBu_4]^+$ counterion. Further evidence of a HB interaction was confirmed by comparing the ^{1}H NMR resonances of the $[NBu_4]^+$ in the starting $[NBu_4][TpMoS(S_4)]$ complex, in which short C–H···S contacts were not observed, to the ^{1}H NMR resonances of the $[NBu_4]^+$ in the $[NBu_4][TpMoS_3]$ product, where shifts of up to 0.65 ppm were observed for $[NBu_4]^+$ resonances. As described later in this review, there are numerous examples of C–H···S–M contacts with sulfur-metal bound species, and many of these may help to stabilize reactive species and promote reactivity in catalysis and enzymatic systems.

Additional evidence for C–H···S HB interactions is supported by a recent study by Wategaonkar and coworkers using both gas-phase vibrational spectroscopy and DFT calculations.[36] Despite the weak nature of both the HB donor and acceptor, C–H···S interactions exhibited all the characteristics of a conventional hydrogen bond, and even displayed binding strengths comparable to more traditional HB in their system. Although S is a less electronegative element than other traditional HB acceptors, S is large and polarizable, allowing it to better participate in dispersion interactions. Indeed, using natural energy decomposition analysis calculations, they found that dispersion was the dominant hydrogen bonding force in all the C–H···S interactions in their system. Importantly, because dispersion is an isotropic component of hydrogen bonding, it is possible that C–H···S HB in the solid state that deviate from linearity are commonly overlooked.

More broadly, other researchers have specifically noted the consequential roles of C–H···S interactions in enzymatic binding pockets. For example, work by Addlagatta and coworkers studying the substrate specificity and catalytic cycle of type 1 methionine aminopeptidase, an enzyme responsible for cleaving methionine from around 70% of proteins in living cells, identified a key C–H HB donor that had been evolutionarily preserved in the enzyme.[37] The authors showed that a hydrogen bond between a S HB acceptor in cysteine and a C–H HB donor in the ε-methyl group of methionine was responsible for the substrate specificity and efficiency in the catalytic cycle. As part of this work, a search of the Protein Databank (PDB) found 20 other instances of C–H···S contacts with a maximum C–S distance of 4 Å between methionine and methionine analogue C–H HB donors in ligands and S-cysteine and methionine HB acceptors. Only a few of the 20 instances were from methionine aminopeptidase enzymes, which suggests a broader generality of this interaction among other types of enzymes and proteins. A separate example comes from a tetrabrachion surface protein isolated from *Staphylothermus marinus*, which exists in black smoker hydrothermal vents where sulfur as S_8 also is present.[38] The crystal structure (PDB: 5JR5) of the tetrameric nanotube encapsulating two S_8 units displays C···S contacts as short as 3.54 Å, suggesting there may also be very short C–H···S stabilizing contacts.

In general, attractive non-covalent interactions with S may be more important than has been previously appreciated. Clearly the interaction of C–H bonds with anionic S H-bond acceptors is expected to be stronger than with neutral analogues; however, these general types of interactions may be significantly more prevalent than commonly recognized. In a review by Meanwell and coworkers[5] that focused on the role of the S σ-hole in S···O, S···N, and S···π interactions in medicinal and organic chemistry, the authors highlight that "because the role of noncovalent interactions involving sulfur in compound conformation and ligand-protein interactions may be underappreciated, this phenomenon may have been overlooked in many drug design campaigns". Similarly, other research on more electron-rich sulfur species has revealed that S···π and S–H···π interactions may be particularly important stabilizing forces in both biological and synthetic systems.[39]

Scope of Review

Inspired by these prior examples pointing to an increased potential importance of non-covalent interactions, we aim to advance the general understanding and appreciation of C–H···S in broad areas of chemistry. To highlight this generality, we analyzed existing data on C–H···S interactions across multiple disciplines using available crystal structure data from the Cambridge Structural Database (CSD). More specifically, we have grouped short C–H···S contacts and into different categories: 1) the S atom coordination number, 2) the types of C–H HB donors, and 3) the S atom oxidation state. In addition, we compare C–H···S interactions when S is bound to an organic molecule or a metal. We present the analysis of these results using 3D histograms and compare these interactions to other established HB acceptors to further cement that C–H···S interactions should not be neglected. Lastly, we provide

selected examples from our own work as well as others that contain previously overlooked C–H···S interactions that may have influenced reactivity and the stabilization of the systems in question. More broadly, this work demonstrates these underappreciated, non-traditional C–H···S HBs are common in molecular biology, catalysis, the primary coordination sphere of inorganic and bioinorganic molecules, and supramolecular systems. The C–H···S motif may even be a distinctive interaction by providing stronger and more selective HB in specific molecular architectures in which non-covalent interactions are used to direct reactivity and/or enhance stability.

C–H···S Interactions

Organic Molecules with Sulfur Hydrogen Bond Acceptors.

C–H···S HBs have higher dispersion character than more traditional HB motifs; therefore, these C–H···S contacts likely have different angle and distance preferences. To better understand these angle and distance metrics, we used available solid-state structural information from the CSD to find all C–H···S contacts with organic-based S HB acceptors. Contacts were restrained to only include instances where the C–H···S (Fig. 1, A1) and H···S---R (Fig. 1, A2) angles fell between 90–180° and H···S (Fig. 1, L1) and C···S (Fig. 1, L2) bond lengths fell between 0–4.0 Å and 0–5.0 Å, respectively. These L1 and A1 parameters encompass a wide array of contacts including weaker interactions, in which A1 is closer to 90° and L1 distances are longer, as well as stronger interactions, in which A1 is more linear and L1 distances are shorter. The L2 and A2 parameters also filter out longer contacts and angles that would not be considered HB interactions.[40] We did not exclude high R-value structures or structures with disorder because it was impractical to identify the proximity of the disorder to the C–H···S interaction sites, but a comparison of the full data set with one filtered to only include R values < 5.0 provided graphically similar results (See SI, and Fig S1). Similarly, we did not filter by H-atom ESDs since the primary goal is to identify trends from these data sets rather than exact bond metrics.

To visualize the > 423,000 C–H···S contacts found in >86,000 structures from this dataset, we plotted a 3D histogram of H···S distance (Å) versus C–H···S bond angle (°) (Fig. 5b). The plot reveals that the majority of C-H···S contacts are not linear. The most common H···S contact is found between 3.12–3.25 Å and 121–126°, which encompasses 6,615 contacts. We expect that most of these structures use the riding model for hydrogen positions and U_{iso}, which may result in shorter C–H distances and thus conservative estimates of C–H···S interactions. Deviations in standard C–H distances or angles are likely to be minor for these types of interactions (see SI). Any HB occurring at this contact angle and distance would traditionally be classified as a weak interaction due to the primary attractive forces being entirely electrostatic and dispersion interactions. Although weak, these inter- and intramolecular forces are additive and can greatly affect the physical and chemical properties of an overall system.[41, 42]

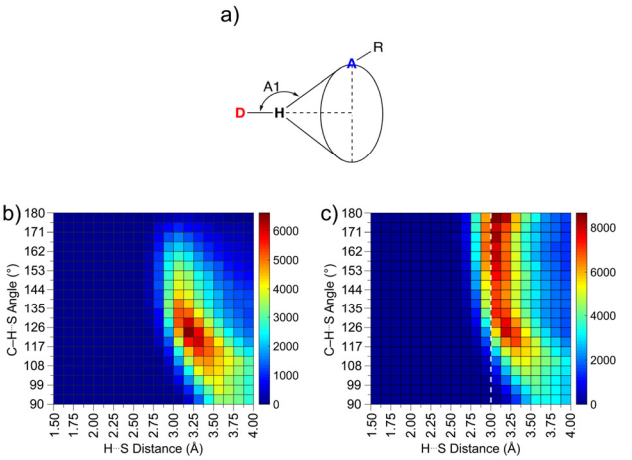

Fig. 5. a) Cone angle of hydrogen bonding. b) 3D histogram visualizing over 423,000 C–H···S contacts identified in the CSD. c) Cone-corrected 3D histogram of all C–H···S contacts. The white dashed line represents estimate of the sum of the van der Waal radii of H and S.

Although a 3D histogram can provide useful information about the most common interaction geometry in the solid state, there is a statistical bias in these analyses due to the HB "cone angle" (Fig. 5a). At a given H···A distance, the acceptor in a D–H···A contact that occurs at exactly 180° can only be located at a singular point in space. When a D–H···A contact angle deviates from linearity, however, there is a geometric cone along the D–H axis that contains identical contact angles around the circumference. As the D–H···A contact angle becomes more bent (*i.e.,* closer to 90°), the circumference of the cone increases, which provides more points in space where the acceptor can be located. This phenomenon means that low angle contacts are statistically more likely to occur and has previously been shown to skew 2D histograms of contact angles of traditional O–H HB systems away from linearity.[43] This statistical bias toward low-angles can be removed by applying a simple cone-angle correction that weights each bin of the histogram by 1/sin(θ), where θ is the C–H···S contact angle. The resultant cone-corrected data effectively removes geometric trends which occur from randomly oriented C–H···S contacts and instead reveals the relative importance and preferred geometry of high-angle contacts in the solid state (Fig. 5c).[44]

The cone-corrected 3D histogram displays a clear geometric preference of C–H···S contacts. Many of the contacts fall below the sum of the van der Waal radii of H and S ($r_w^H + r_w^S$, estimated as a white dashed line in Fig. 5c).[45] At these shortest distances (< 3.00 Å), high-angle contacts are favored, revealing an attractive interaction promoting linear contacts. Even at distances greater than the sum of the van der Waals radii, the C–H···S contacts show strong geometric preferences. For example, there is a preference for linear contacts between 3.00–3.13 Å, and as the distance increases (3.12–3.63 Å), the low-angle contacts become equally or more important than high-angle (linear) contacts. Finally, at longer distances (3.62–4.00 Å) the angle dependence decreases, and it is less likely that strong, directional HB occurs at these distances; instead, we see more random, geometrically- and statistically-driven contacts,

more reminiscent of interactions dominated by dispersion interactions.[46, 47]

As an example of such C–H···S interactions impacting structural outcomes, we have re-assessed work from our own group to identify previously overlooked C–H···S contacts that likely contribute to the observed solid-state structure. In 2016, one of our groups prepared a tetrameric disulfide cyclophane (Fig. 6), which surprisingly folded in on itself and form several strained C–S–S–C torsional angles rather than bind a solvent or small guest molecule. Reanalysis of this structure revealed a very short, linear intramolecular C–H···S contact (2.81 Å, 170°, highlighted in Fig. 6), which likely contributes to the compact structure. Further analysis also identified three additional intramolecular C–H···S contacts with longer H···S distances of 3.68–3.94 Å. These distances, however, fall within the region of the weighted histogram that shows little contact angle preference, and so are likely not forming a HB. Finally, we identified 27 intermolecular contacts with C–H···S angles ranging between 101 and 175° and H···S distances of 2.81–3.89 Å, which may help stabilize the overall compact packing of the macrocycle in the solid state.

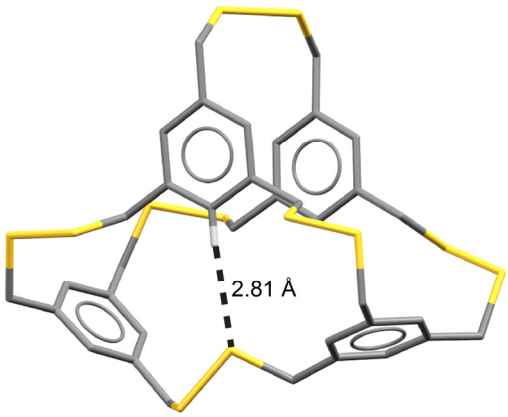

Fig. 6. A relatively short and linear C–H···S contact in a disulfide cyclophane may help stabilize strained torsional angles.

S HB Acceptors with Traditional HB Donors

Comparing the cone-corrected 3D histograms of S contacts with traditional N–H (Fig. 7a) and O–H (Fig. 7b) donors shows different interaction profiles. C–H HB donors show flexible geometric preference for high- and low-angle contacts and support a wide range of H···S distances, whereas N–H and O–H HB donors are only found in a narrow geometric window. These traditional N–H and O–H HB donors prefer to only make short and linear contacts with few examples in the CSD showing deviations from this idealized geometry. These data suggest that the HB interaction between S and traditional N–H and O–H HB donors is generally stronger than with C–H HB donors and has more charge-transfer character due to the observed short distances and linear contact angles. The data also show, however, that C–H···S interactions, which have more dispersion character, display more contacts at long distances and with bent contact angles when compared to N–H and O–H HB donors. In a computational study, Flood and coworkers showed that C–H hydrogen bond donors start to show greater stabilization of Cl^- than NH donors at longer contact distances.[48] In combination with our analyses, which show a lower preference for linear C–H···S interactions, C–H···S interactions seem to outperform N–H and O–H HB donors at long distances and more bent contact angles.

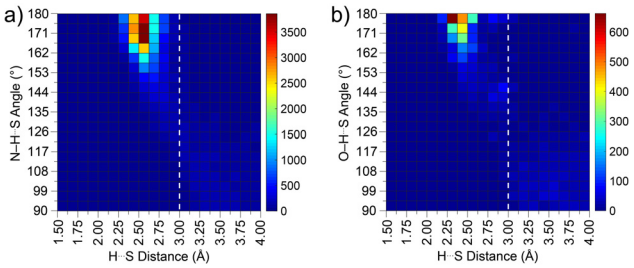

Fig. 7. 3D histogram of a) N–H and b) O–H hydrogen bond donors with S.

Comparing HB Acceptors

We also analyzed the C–H···A contacts with other HB acceptors from neighboring elements on the periodic table (N, O, F, P, Cl, Se, Br, Te, I) (Fig. 8). Using the same search criteria as for sulfur, we found that oxygen had the greatest number of inter- and intramolecular contacts (7,898,338 contacts in 562,725 structures), followed by F (3,540,975 contacts in 111,861 structures)), Cl (1,338,770 contacts in 103,437 structures), and N (1,082,175 contacts in 210,473 structures), perhaps suggesting that the acceptance of C–H HB with O, Cl, and N may be in part due to their ubiquity in solid-state structures. Comparison of the resultant histograms shows that the flexible contact angle geometry of the C–H HB donor is conserved. In addition, almost all C–H···A contacts occur at distances greater than 2.2 Å, which is significant because contacts greater than this distance have generally been defined as weak HBs with mostly electrostatic and dispersion character by Jeffrey[49] and later Steiner.[43] Although these data do not allow for determination of the absolute strength of these interactions, we used distances and contact angles inspired by Jeffrey and Steiner to broadly categorize ‘strong’, ‘moderate’, and ‘weak’ C–H···A interactions (Table 1). C–H···A contacts that fall in the region of the cone corrected 3D histogram that shows little preference for either high- or low-angle contacts are likely not being driven by significant attractive interactions.

Table 1. Parameters used to broadly categorize C-H HB as strong, moderate, and weak. Distance and angle ranges are inspired by analyses of hydrogen bonding in the solid state by Jeffrey and Steiner.[43, 49]

	Strong	Moderate	Weak
H···A Distance	$\leq r_w^H + r_w^A$	$> r_w^H + r_w^A$	$> r_w^H + r_w^A$
C–H···A Angle (°)	> 130	> 130	> 90

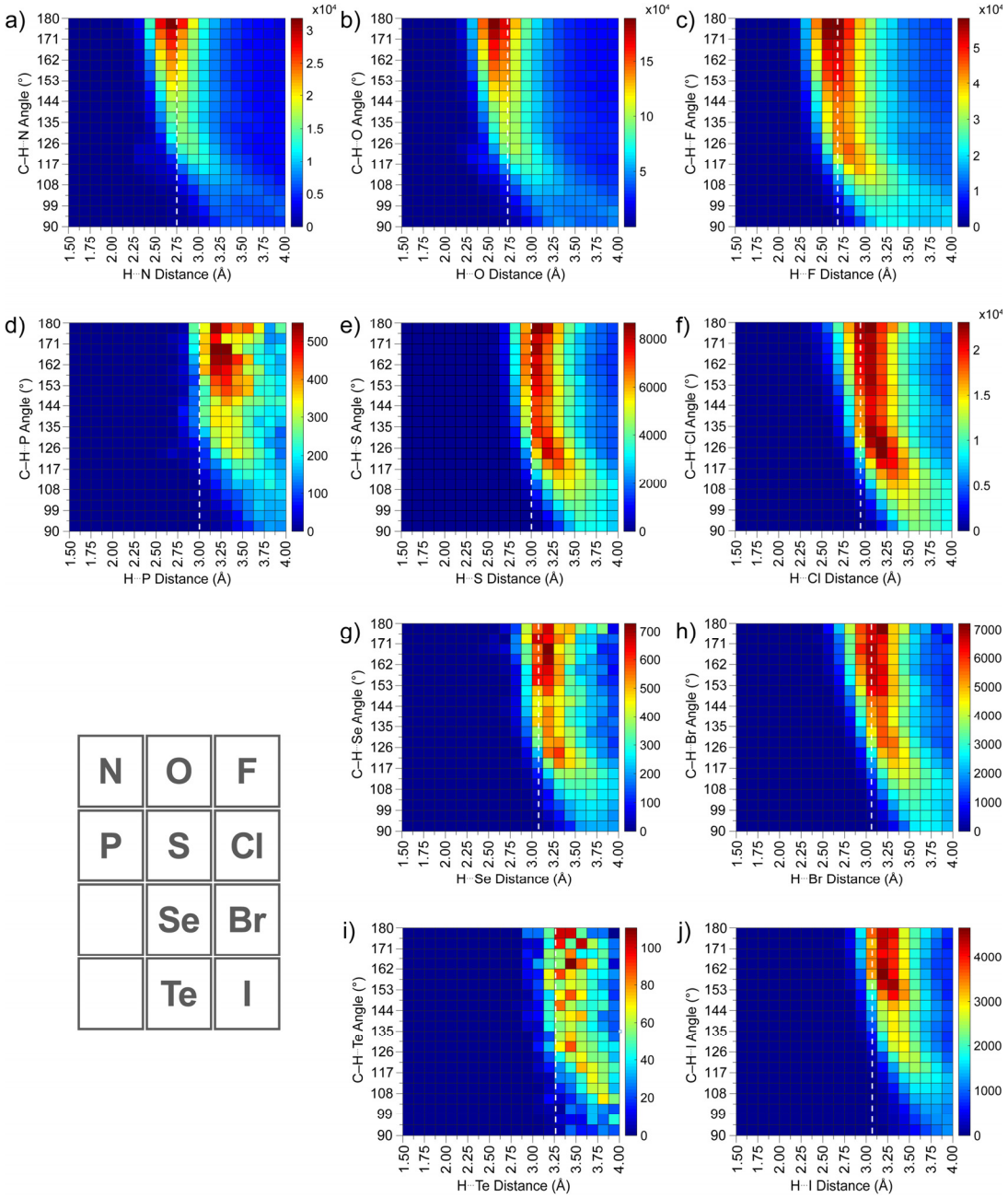

Fig. 8. Cone-corrected 3D histograms of C–H…A contacts found in the CSD with a) N, b) O, c) F, d) P, e) S, f) Cl, g) Se, h) Br, i) Te, and j) I. White dashed line represents estimate of the sum of the van der Waal radii of H and A.

The second-row elements N, O, and F are among the smallest, least polarizable, and most electronegative atoms (Fig. 8a-c) and the weighted 3D histograms of these elements show the highest proportion of strong HB contacts. This driving force toward short contacts, however, makes these elements poor C–H HB acceptors at longer distances. An example of this point is highlighted in work studying the *cis/trans* isomerization in amide and thioamide containing peptoids.[50] The authors found that a C–H···S interaction in the thioamide derivative caused a greater preference for the *cis* conformer in the thioamide when compared to the amide derivative. A crystal structure of the thioamide showed a key intramolecular C–H···S HB with a bond distance of 2.9 Å (Fig. 9), which is a strong C–H···S HB but much longer than most C–H···O interactions. Despite generally being a weaker HB acceptor than O, the S-containing thioamide formed a strong HB over the greater distance whereas the O-containing amide could not (S is a larger element than N, O, and F, which facilitates longer C–H contacts). In addition, the weighted 3D histograms reveal that S, much like Cl, is more likely than the second-row elements to make contacts at distances longer than

the sum of the van der Waal radii. This observation is further reflected by work from the Shimizu group, which shows that S-π interactions are more favorable than O-π interactions at long distances.[39]

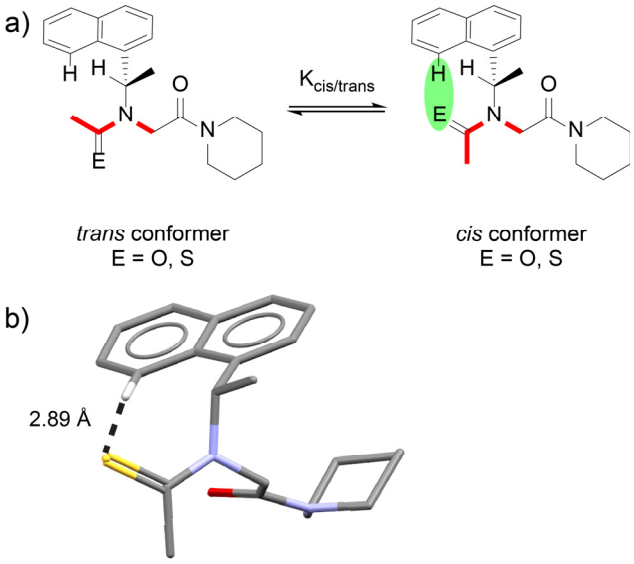

Fig. 9. a) *cis/trans* Isomerization of synthetic peptoids. A C–H···A HB helps favor the *cis* conformation. b) The crystal structure shows a strong C–H···S HB in the solid state that helps favor the *cis* conformation in the thioamide derivative.

The propensity for S acceptors to make longer contacts with C–H donors than those that are typically observed for N, O, and F may contribute to prior underappreciation of C–H···S interactions. For example, Goel and coworkers found that inter- and intramolecular C–H···N and C–H···O HBs were crucial in the aggregation induced emission (AIE) mechanism for a novel class of luminogens (Fig. 10). Studying the published crystal structure, we also find highly linear C–H···S contacts (178°) that may assist in rigidifying the aggregates. The C–H···S contacts were found at a much longer C–H···A distance (3.19 Å) than the other C–H contacts to O and N in the structure (2.52–2.58 Å).[51] Other work by Tang and coworkers supports this possibility, showing that strong, linear C–H···S HB contribute to AIE in their systems.[52]

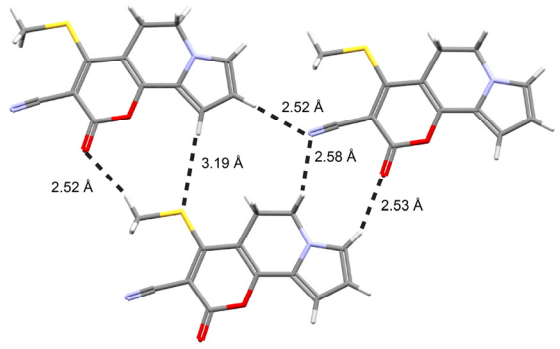

Fig. 10. a) Crystal packing of the luminogen reveals C–H···O (atom denoted in red), C–H···N (blue) and C–H···S (yellow) intermolecular C–H HBs.

Although the second-row elements favor short contacts, the rest of the HB acceptors in the third, fourth, and fifth-rows tend to make moderate-to-weak contacts. In this regime, as the electronegativity of the HB acceptor decreases, more linear C–H···A contacts are favored. This trend is best seen in third row elements P, S, and Cl. Chlorine, the most electronegative atom in this series, has the highest number of weighted low-angle contacts and P, the least electronegative atom in this series, has the lowest. This across-row trend also holds true for the small, electronegative second-row elements. From the third-row down, we also see that this trend holds down a periodic column, which is best visualized by comparing Cl, Br, and I. Cl, the most electronegative atom in this series, again has the greatest number of weighted low-angle contacts, whereas I, the least electronegative in this series, has the least. To explain this trend, we have to consider each attractive force in a HB. The attractive interaction from charge transfer decreases the fastest over distance (diminishing approximately as e^{-r}), and therefore cannot explain the trends in the weak-to-moderate contacts that extend past the sum of the van der Waal radii of H and A. Electronegativity does not increase the preference for linearity, so electrostatic interactions also likely do not explain the trends. Furthermore, dispersion interactions are isotropic so would not be expected to favor specific contact angles. Therefore, polarizability, which is the ability of the HB acceptor to redistribute its electron density, must be the most important acceptor character driving linear contact angles. This observation would also explain why the second-row elements, which are small, and not very polarizable, behave differently from the rest of the acceptors.

The chalcogens S and Se have generally been considered to be poor HB acceptors due to their low electronegativity. Both these elements, however, are polarizable and therefore are more likely to be C–H HB acceptors. C–H···S/Se contacts behave similarly, with a strong preference for linear contacts and a weaker preference for low-angle contacts. Even Te appears to show a preference for linear contacts, although there are far fewer of these examples (3,677 inter- and intra-molecular contacts), perhaps reflecting the synthetic challenges working with this highly reactive element. Nevertheless, there are two published examples specifically referencing the importance of C–H···Te interactions.[53, 54] The most recent example, published in 2020, studied the C–H···A interactions of a series of *bis*(silanechalcogenones). Using evidence from crystal structures and computations, the authors found that S made the strongest C–H HB bonds compared to Se and Te; however, the size of Te allowed it to make both inter- and intramolecular HBs. Given that the weighted 3D histogram of C–H···Te contacts reveals a preference for linear geometries, perhaps there are already examples of these contacts that have been previously overlooked.

Finally, we note the striking similarity between the behavior of C–H···S contacts and C–H···Cl contacts. Cl is a well-established C–H HB acceptor. The S and Cl contacts occur at similar distances, but S is a more polarizable element and should act as a better C–H HB acceptor. Consistent with this logic, we see

more of a linear preference in S contacts when compared to Cl. If C–H···Cl HBs have been identified as salient non-covalent interactions, C–H···S HB should be equally established.

S Coordination Number

The number of atoms that S is bonded to, defined here as the coordination number, can affect the electrostatic and steric environment as well as the polarizability of the HB acceptor, which should in turn change the nature of the C–H···S interactions. Indeed, the weighted 3D histograms of C–H···S contacts when S is bonded to one (SR), two (SR_2), and three (SR_3) other non-metal atoms reveal major differences in the important contact geometries (Fig. 11). When the S HB acceptor is bonded to one other atom, the contacts are shorter and more linear, perhaps due to less steric crowding around the S HB acceptor. Regions of both high-angle and low-angle contacts are important when S is bonded to two other atoms, and most contacts are moderate to weak.

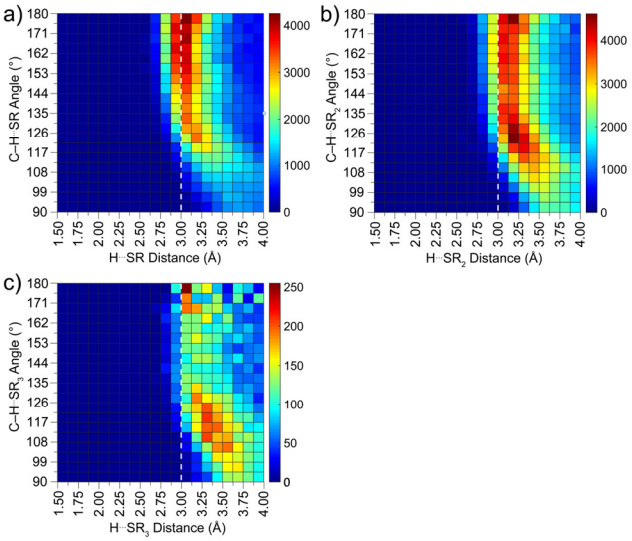

Fig. 11. Cone-corrected 3D histograms of S bonded to a) one non-metal atom, b) two non-metal atoms, and c) three non-metal atoms.

Although we cannot definitively identify why bent interactions are favored in SR_2 and SR_3 contacts, we can see evidence of their importance in published examples. For example, in 2017 Anderson and coworkers reported an unexpected attractive interaction between a pyridine ligand and the alkyl straps in sulfur-strapped Zn-porphyrins.[57] 2D NMR spectroscopy, UV-vis spectroscopy, and crystal structure analysis revealed the formation of both an expected *out* isomer (Fig. 12a) and also an unexpected, more sterically hindered *in* isomer (Fig. 12b). The formation of the *in* isomer is attributed to C–H···π interactions between the alkyl C–H groups on the strap and the pyridine ring. The authors also comment that "there may also be an attractive interaction between the sulfur atom and the α C–H of the pyridine." Investigating the published crystal structure, we clearly see that although the C–H···S contacts are bent, one falls squarely in the region of important low-angle C–H···S contacts with an H···S distance of 3.14 Å and a C–H···S contact angle of 124°.

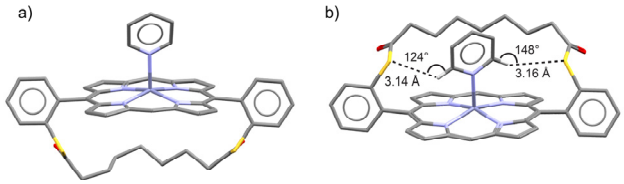

Fig. 12. a) *Out* isomer and b) *in* isomer of sulfur-strapped Zn-porphyrins.

Alkyl vs. Aryl Based C–H donors

In general, the C–H atoms of carbons with more *s*-character are more acidic and are better HB donors. When comparing cone corrected 3D histograms of alkyl and aryl C–H HB donors, however, we observed that linear contacts are more important with alkyl C–H HB donors whereas low angle contacts are more important with aryl C–H HB donors (Fig. 13). Even though this outcome may at first seem counter-intuitive, it may reflect that aryl C–H HB donors are better at accommodating bifurcated hydrogen bonds than alkyl C–H donors. For example, we found that about 37% of C–H···S contacts with aryl C–H HB donors are bifurcated between two adjacent aryl C–H HB donors. A 3D histogram of just these bifurcated C–H···S···H–C contacts (Fig. S5) shows a strong preference for the same low-angle contacts that are observed for all aryl C–H···S contacts.

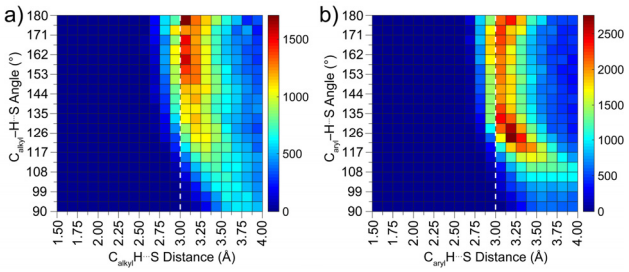

Fig. 13. Cone-corrected 3D histograms of C–H···S contacts with a) sp^3 alkyl C–H HB donors and b) sp^2 aryl C–H HB donors.

Alkyl and aryl C–H HB donors are not relegated to synthetic systems, and there is also evidence for both sp^3 and sp^2 C–H HB donors interacting with S in biological systems. For example, we revisited the crystal structure of the first discovered bacterial ion channel for HS^- and found C···S contact distances between valine and leucine amino acids and HS^- that were about the same distance or shorter than the majority of weighted C–H···S contacts (Figs. 14 and 5a).[58] In addition, we found evidence of both sp^3 and sp^2 C–H HB donors from threonine and tryptophan residues in streptavidin in contact with the thioether (Fig. 15). The streptavidin-biotin complex is one of the strongest non-covalent binding events known in nature, in part due to the high geometric complementarity of the host-guest complex and a high degree of hydrogen bonding.

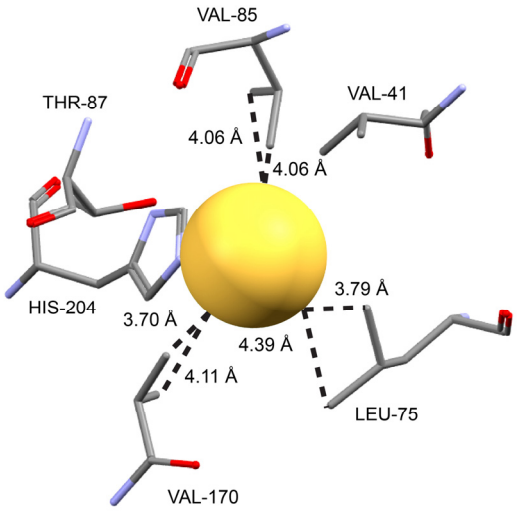

Fig. 14. Leucine and valine amino acid residues in contact with HS^- in the first discovered bacterial ion channel for HS^-. The labeled lengths correspond to C–S distances. (PDB: 3TDX)[59]

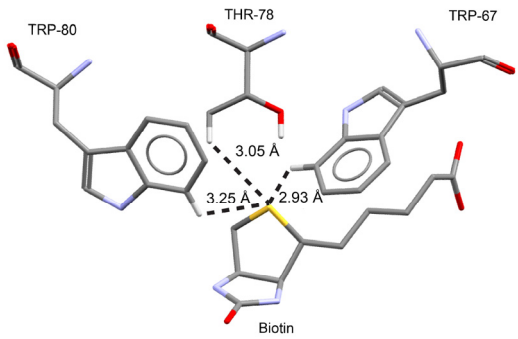

Fig. 15. Tryptophan and threonine amino acid residues in contact with the biotin thioether in the streptavidin-biotin complex. (PDB: 6M9B)

Hydrogen Bond Acceptor Directionality

Geometric preference of hydrogen bonding in the solid state also extends to the HB acceptor. Strong HB often have clear R---A···H acceptor directionality (A2, Fig. 1), whereas weak HB lose this directionality. For example, the acceptor directionality in a strong HB may be driven by the required geometry of charge transfer or electrostatic potential. On the other hand, a weak HB with high dispersion character would lose much of its directionality.

The acceptor directionality in both linear and bent C–H···S contacts can be visualized by using a 3D histogram of C–H···S contact angle vs. R---S···H contact angle in which both axes of contact angles are weighted by the cone angle correction (Fig. 16e). These bi-weighted 3D histograms do not show the most common donor and acceptor contact angles, but rather show what combinations of C–H···A and R---A···H angles are particularly important geometries. For example, at C–H···S angles between 90° and 95° there is no preferred R---S···H directionality, meaning that each bin should have about the same low importance. These contacts are either statistically-driven or are van der Waals contacts. On the other hand, C–H···S angles between 175 and 180° either prefer a linear R---S···H acceptor angle or a bent acceptor angle between about 108–126°. As the C–H···S bond angle deviates farther from linearity, specific acceptor directionalities start to lose importance, perhaps reflecting the increasing dispersion contribution to hydrogen bonding at bent contact angles.

Most HB acceptors with C–H HB donors favor a highly linear acceptor directionality and only occur at linear C–H···A contact angles (Fig. 16). As the C–H···A angle deviates from linearity, preference for any acceptor directionality gradually disappears. Sulfur is the exception to this trend. Sulfur HB acceptors show an 'island' of important R---S···H angles at low-angle C–H···S contacts. Although the donor directionality in this island is weak, S is the only HB acceptor that shows any acceptor directionality for this bent, weak HB. This unique geometry is completely removed with SR acceptors (Fig. S6), and is exaggerated with SR_2 acceptors (Fig. S6b). Notably, this geometry is not seen with OR_2 acceptors (Fig. S6a), but is present with SeR_2 acceptors (Figure S6c). Because there is some (albeit weak) attractive interaction or environment that is promoting this unique contact geometry, S may be a stronger C–H HB acceptor at bent angles compared to other acceptors.

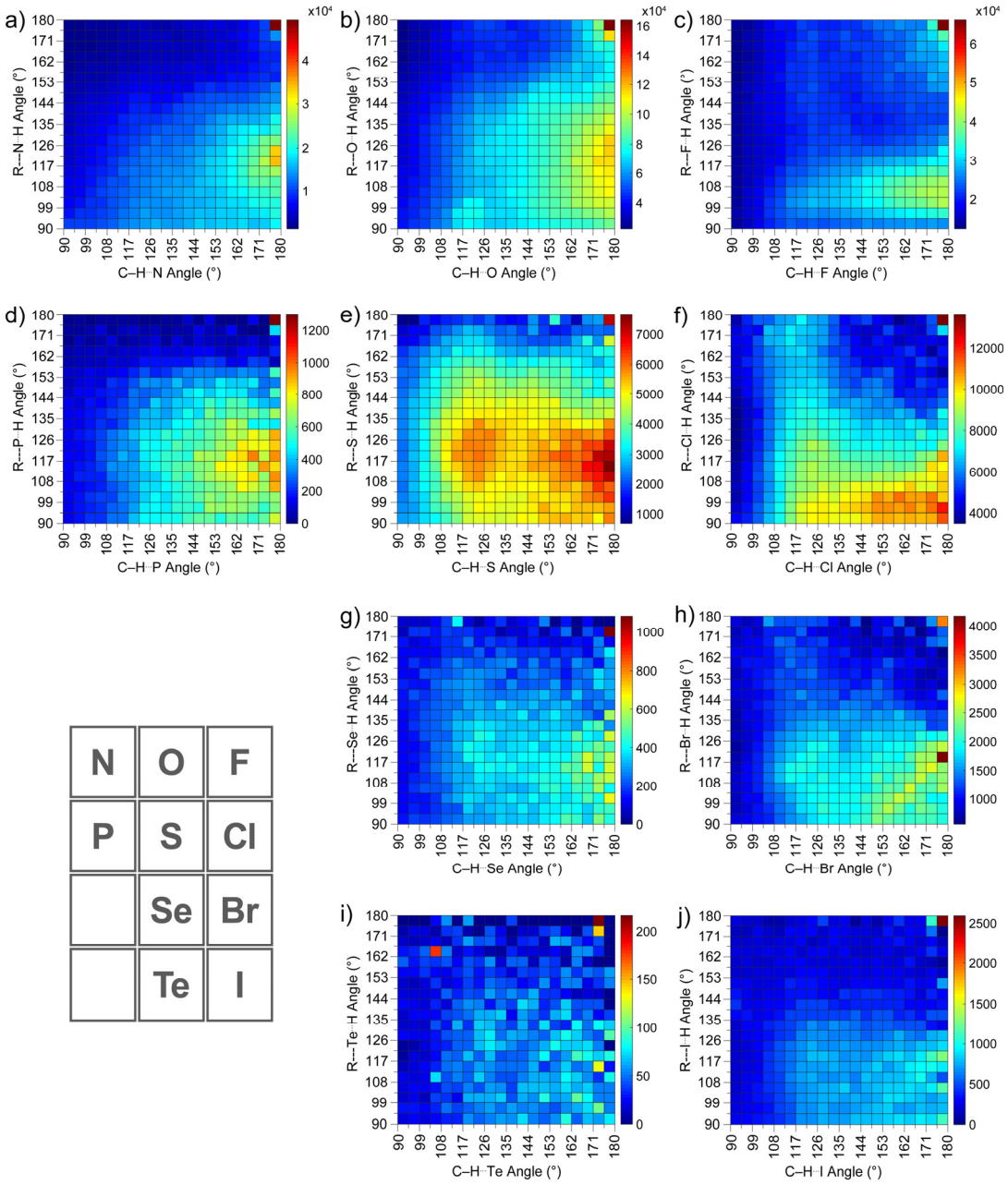

Fig. 16. Bi-weighted 3D histograms of C–H···A contacts found in the CSD with a) N, b) O, c) F, d) P, e) S, f) Cl, g) Se, h) Br, i) Te, and j) I.

Sulfur Hydrogen Bonding Interactions in Metal Sulfur Ligated Complexes

Similar to the established hydrogen bonding interactions between sulfur as a HB acceptor with N–H and O–H HB donors in organic molecules, sulfur atoms coordinated to metal centers also participate in hydrogen bonding. S donor ligands are widely known in many subfields of inorganic chemistry ranging from the active site of bioinorganic cofactors, such as nitrogenase, to catalytic systems. Model systems have highlighted how certain R–H···S HB motifs can be consequential in catalytic turnover and reactivity. An example from Riordan and coworkers in 2003 focused on investigating sulfur alkylation rates by functionalized zinc thiophenolates in the presence of *ortho* and *para* N–H amide HB donors.[60] In this work, the second-order rate constants for the alkylation of functionalized zinc thiophenolates with BnBr in the presence of *ortho* and *para* N–H amide HB donors were 1.3 x 10^4 and 44 x 10^4 $M^{-1}s^{-1}$, respectively. The different rates were attributed to stabilizing *ortho*-N–H HB donors significantly diminishing the nucleophilicity of the bound thiophenolates. This interaction

was confirmed by ^{1}H NMR and IR spectroscopy and observed by the short N–H···S distance in the solid state with a H···S bond distance of 2.49(2) Å. The authors speculate that similar R–H···S HB interactions may play a role in other zinc thiolates of metalloproteins.

Establishing C–H HB interactions with atoms in the primary coordination sphere of metal complexes is a contemporary approach to modify the stability and properties of different metal complexes. In an elegant recent example, functionalization of the 2-position of a phenanthroline (phen) ligand with –CF_2H, a known C–H HB donor with similar donating strength to amines and thiols,[61] generated directional close contacts between the CF_2H group and the primary coordination sphere of the metal. Szymczak and coworkers synthesized complexes of Pd (PdX_2(phen) where X = F, Cl, Br, and OR) and showed a C–H···X HB interaction between the CF_2H group and the X-type ligand in the primary coordination sphere of the Pd complex (Fig. 17).[62] These results were shown by solid state structural analysis and confirmed by spectroscopic data and computational studies. Hydrogen bonding interactions with H···O distances were as short as 2.002 Å. Furthermore, an interesting result from this work showed that while the CF_2H group is a great HB donor, the $CH(CH_3)_2$ group is also capable of providing stabilizing HB interactions. Both $PdCl_2$(phen) complexes where an *ortho*-CF_2H and *ortho*-$CH(CH_3)_2$ of the phen ligand were synthesized and comparative bond lengths of the C–H···Cl interaction were observed with distances of 2.34 and 2.50 Å for *ortho*-CF_2H and *ortho*-$CH(CH_3)_2$ complexes, respectively. These complexes were stable under strong reducing agents and bases, demonstrating the utility of C–H HB donors in the primary coordination sphere, whereas traditional hydrogen bond donors, like OH groups, are reductively unstable and can be deprotonated.

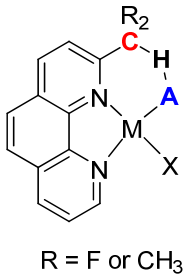

Fig. 17. C–H hydrogen bonding interactions in the primary coordination sphere of metal complexes as demonstrated by Szymczak and coworkers.

To expand the analysis of C–H···S HB interactions in organic molecules (*vide supra*), we searched for HB interactions involving C–H···S–M motifs where S is bound to a metal. This analysis knits together work by others that highlight the importance of HB through influencing model chemistry of metalloenzymatic reaction pathways through N–H···S HB and the ability of C–H HB donors to form C–H···X–M HB interactions in the primary coordination spheres of metal complexes. Similar to the metal sulfur interactions observed in organic compounds, we focused on CSD search parameters for C–H···S–M contacts to included C–H···S (A1) and H···S–M (A2) angles of 90–180° and H···S (L1) and C···S (L2) bond lengths of 0–4.0 and 0–5.0 Å, respectively (Fig. 18). Our initial searches aimed at determining whether short C–H···S–M contacts are common in *d*-block metals and any bound sulfur ligand.[63] The results of the initial search provided 45,733 molecules that fit these parameters and a total of 487,171 intra- and intermolecular C–H···S–M contacts (Fig. 19a). The high number of contacts observed per molecule may be due to the fact that organic ligands are often in close proximity to the primary coordination sphere, thus favoring potential interactions.

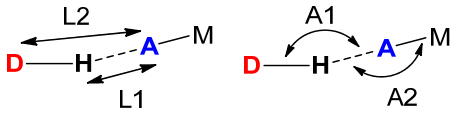

Fig. 18. Lengths and angles referred to in this section, where the HB acceptor (A) is bound to a metal.

The cone corrected 3D histogram for the C–H···S–M contacts for *d*-block metals reveals that the majority of the weighted contacts include bond lengths between 3.00–3.25 Å at angles > 144°, with notable 'islands' of favorable contact geometry at lower angles of 12–135° and at longer distances of 3.00–3.38 Å. We also compared C–H···Cl–M HB contacts based on the similarity of Cl and S as well as prior work demonstrating the importance of C–H···Cl–M interactions. Cl and S are nearly identical in size with van der Waals radii of 2.05 and 2.06 Å, respectively,[64] so a comparison of these H···Cl contacts would validate the observed H···S seen in Fig. 19 as HB interactions. The cone corrected C–H···Cl–M contacts plotted in Fig. 19b show data from 77,677 molecules with 920,886 inter- and intramolecular contacts. The major difference between the plots of Cl and S HB contacts is that Cl HB contacts are more consolidated above 100° and at distances between 2.75–3.00 Å. These data suggest that C–H···Cl–M contacts may be stronger and more directional than C–H···S–M contacts, and may be attributed to higher steric bulk of thiolates in comparison to bound Cl in coordination complexes, or to slight differences in the dipole moment between Cl and S due to the greater electronegative of Cl. We note that such discrepancies between Cl and S HB contacts are not observed when A is not bonded to a metal. Differences between Cl and S may also be attributed to their valency. Chloride is a monovalent ligand, whereas sulfide-based ligands are divalent and the ability for a shorter and more directional HB interaction for Cl could be due to steric interactions. The similarities in shape and localization of areas with high frequency in Fig. 19 do suggest that Cl and S behave similarly as HB acceptors despite a weaker interaction with S. Lastly, the cone corrected 3D histogram of C–H···S contacts where the S atom is bonded to a metal (Fig. 19a) and non-metal (Figs. 5c and 8e) look strikingly similar. The majority of the contacts include bond lengths between 3.00–3.25 Å at angles >135°, which further validates that both organic molecules and metal complexes engage in C-H···S HB interactions.

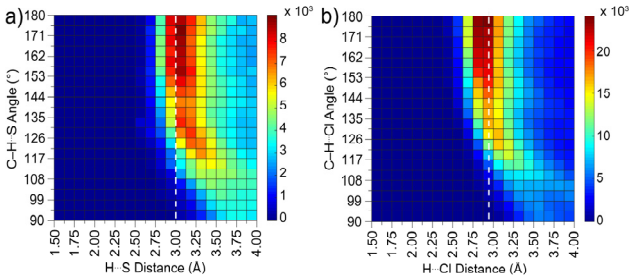

Fig. 19. Cone corrected histograms of a) C–H···S–M, and b) C–H···Cl–M contacts in *d*-block metals where S or Cl are in the primary coordination sphere. The white line for each plot indicates the sum of the van der Waal radii between A and H.

We next aimed to identify if certain groups in the *d*-block contained more C–H···S–M contacts than others. In comparison to nitrogen and oxygen, S is relatively large and polarizable, and so we expect that complexes with the more polarizable late transition metals will have greater affinity for thiolate and S-bound ligands, resulting in more HB contacts. A survey of groups 3-12 from the periodic table confirms that early transition metals have far fewer C–H···S–M contacts in comparison to groups 7-12. Cone corrected 3D histograms are shown for groups 7-12 (Fig. 20). The group with the shortest C–H···S–M contacts was group 10, which included 11,986 molecules with 96,423 inter- and intramolecular contacts. As we move from left to right in the periodic table across the *d*-block elements, a trend emerges where the most concentrated or highest frequency of weighted C–H···S–M contacts occurs with less directionality.

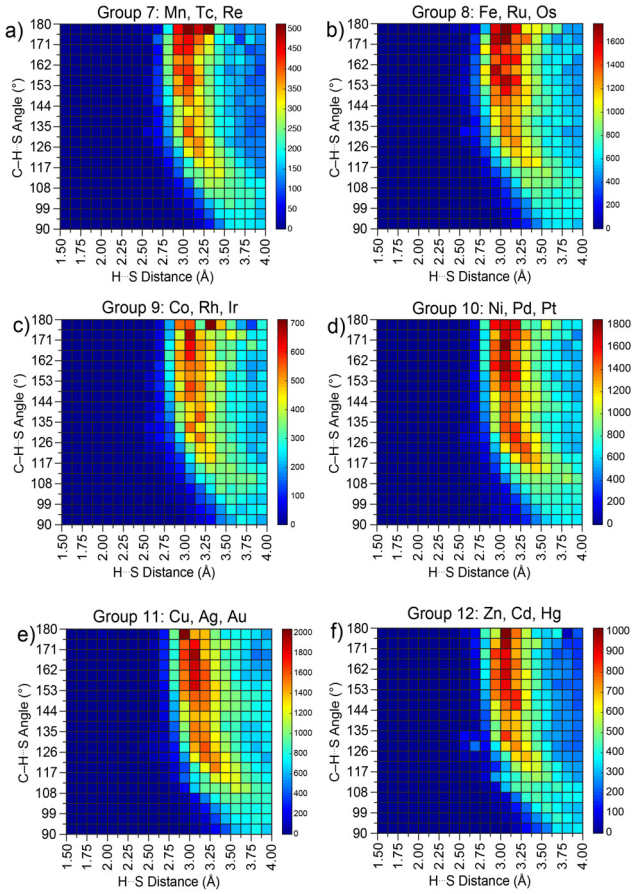

Fig. 20. Cone corrected histograms of C–H···S–M of groups a) 7, b) 8, c) 9, d) 10, e) 11, and f) 12 of the transition metals.

For group 1 metals, only 170 molecules matched the search criteria. Although there were regions of increased C–H···S–M contacts near 3.12 Å and angles above 155° the small data set does not allow for further analysis.[65]

Structures Exhibiting Short C–H···S–M Contacts

With the designation of H_2S as the third gasotransmitter, extensive research has focused on understanding its role as a signaling molecule, transport throughout biological systems, and reactivity with metalloproteins.[66-70] The bivalve mollusk *Lucina Pectinata*, a species of clam found in sulfur rich environments, binds hydrosulfide with high affinities. We revisited the HS^--bound hemoglobin I (HbI) structure determined in 1994 by Bolognesi and coworkers.[71] The active site revealed what is now referred to as the "Phe cage", which is a hydrophobic pocket around the HbI, and a glycine residue that is a hydrogen bond acceptor to HS^- to further stabilize the reactive HS^- anion. In tandem, the Phe cage, which is believed to prevent water molecules from displacing the bound HS^-, and the glycine residue, which aids in HS^- coordination, are the thought to be the major contributing factors for the high binding affinities of HS^- to the Fe center. Reanalysis of the structural data of sulfide-bound HbI from *L. Pectinata* showed that there is a short C···S contact of 3.9 Å between the Phe-43

residue and the S atom bound to Fe. Although the H atom on the metal sulfide was not located, the short C···S distance suggests that the H···S distance could be as short as 2.8 Å, which would be considered one of the stronger C–H···S–M contacts according to the data collected by Bolognesi shown in Fig. 21a (PDB: 1MOH).

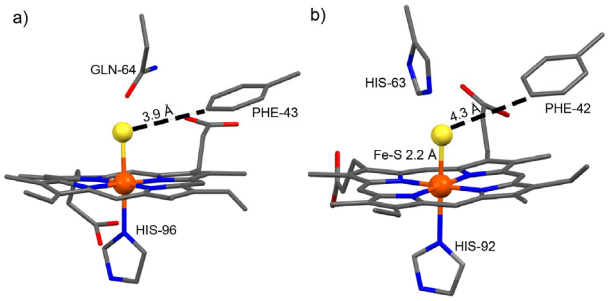

Fig. 21. X-ray structures of a) sulfide bound Hb1 isolated from *L. Pectinata* and b) sulfide bound Hb isolated from human Hb. The labeled lengths correspond to C–S distances.

Later work by Banerjee and coworkers discovered that myoglobin can support catalytic H_2S oxidation to form thiosulfate and polysulfides prompting further investigation of how sulfide binds human Fe porphyrins.[68] In subsequent work focused on structural and mechanistic insights into this process, the crystal structure of sulfide bound human hemoglobin (Hb) was reported (Fig. 21b, PDB: 5UCU).[72] There are key differences in the active site between the sulfide bound Hb structures from *L. Pectinata* and humans. In human Hb, the hydrogen bond acceptor to the bound sulfide is His rather than Gly in *L. Pectinata*. In addition, the Phe residue in the human Hb has a longer C···S contact at 4.3 Å, which would suggest a weaker C–H···S–M interaction. Single site mutagenesis of Hb1 from *L. Pectinata* has been used to understand how H_2S oxidation is affected by the hydrophobic pocket of *L. Pectinata*.[73] When the Phe residues are modified with more polar, hydrogen bond accepting residues, which are more similar to those of human Hb, the rate of H_2S oxidation is increased. Based on the short, potentially strong C–H···S contact in the primary coordination sphere of sulfide bound to Hb1 from *L. Pectinata,* we postulate that these short stabilizing contacts may contribute to the slowed rate of sulfide oxidation. It is possible that the C–H···S–Fe hydrogen bond causes the bound sulfide to be less readily oxidized by Fe due to an attractive force between the partial negative charge on S and the partial positive charge of the hydrogen atom involved in hydrogen bonding, thus limiting its reducing power and slowing down the oxidation process.

Stabilizing interactions within other metal hydrosulfide complexes by C–H···S–M interactions were also found when using the same search criteria for C–H···S–M contacts of the *d*-block. Searching the CSD for short contacts for structures in which the S HB acceptor was a M–SH moiety revealed 202 molecules with 1,476 contacts (Fig. 22). The cone corrected 3D histogram shows the majority of contacts have an angle greater than 150° at distances < 3.12 Å. Such interactions, which include the example from *L. Pectinata*, would be considered to be moderate in strength.

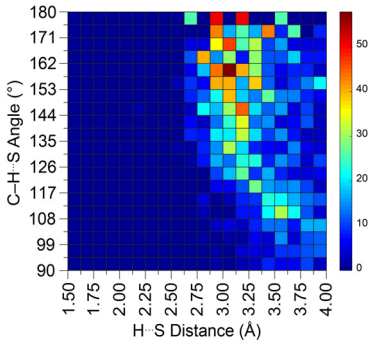

Fig. 22. Cone corrected histograms of C–H···(SH)–M with *d*-block metals.

Zn–S complexes are widely studied in biological sulfur chemistry due to the known affinity for the formation of Zn–S bonds, such as in Zn finger proteins. Zn–SH have been demonstrated to form through ligand metathesis reactions of Zn–OH with H_2S, leading others to study the reactivity of these compounds as models in biological reactivity. For example, Galardon and Artaud have studied *tris*(pyrazol)boratezinc hydrosulfide (TpZnSH) species, in which the TpZnOH precursors are structurally similar to the carbonic anhydrase active site, to further understand their roles in persulfidation reactivity *via* Zn–SH intermediates.[74] In this work, an isopropyl functionalized Tp ligand (^{iPr}Tp) is used to isolate a ^{iPr}TpZnSH complex. Further inspection of this structure shows multiple short C–H···S–Zn hydrogen bonding interactions (Fig. 23). All three isopropyl groups of the ^{iPr}Tp ligand show the tertiary C–H bond pointing towards the bound Zn–S. The H···S bond lengths and C–H···S bond angles are 3.07, 3.11, 3.29 Å and 151, 154, 136°, respectively. The Zn–S bond distance is 2.23 Å and slightly shorter in comparison to some other Zn–SH species where C–H···S hydrogen bonds are weaker.[75]

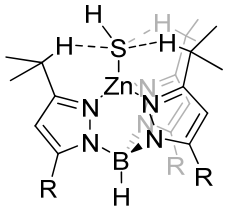

Fig. 23. Graphical representation of C-H···S-Zn hydrogen bonding interactions observed in a ^{iPr}TpZnSH complex.

Conclusions

This review summarizes evidence for HB interactions between C–H bonds as hydrogen bond donors and S atoms as hydrogen bond acceptors. Although specific C–H···S hydrogen bonds have been documented previously in selected systems, this review highlights that these close contacts are significantly more common than typically appreciated. This generality is supported by the tens of thousands of solid-state structures

with C-H···S interactions. Following the standard definition of a HB, we establish that C–H···S close contacts are indeed HB interactions, with the most defining factor being the distance between a H atom and the acceptor. Such contacts in both organic molecules and metal complexes with S in the primary coordination sphere were used to construct 3D histograms to visualize these trends for preferential distances and angles for C–H···S close contacts.

Based upon our findings in the CSD searches we can now summarize the nature C–H···S close contacts:

- Cone corrected histograms for C–H···S contacts where S is bound to a non-metal show a geometric preference for contacts at angles > 155° and distances between 2.83–3.13 Å.
- Cone corrected histograms for C–H···S contacts where S is bound to a metal show identical geometric preferences for contacts at angles >155° and distances between 2.83–3.13 Å.
- Cone corrected histograms for C–H···X contacts (where X = Cl or S, and X is bound to a metal or non-metal) are strikingly similar, which supports the strong similarity between Cl and S.
- Acceptor polarizability is an important contributor toward linear contact angle preference.
- Specific examples from the literature indicate overwhelming evidence for C–H···S hydrogen bonding interactions.

These analyses demonstrate that C–H···S HBs out-perform more traditional N–H···S and O–H···S HBs at long distances and bent contact angles. This marked difference in contact angle geometry and distance may help explain why C–H···S contacts have been traditionally overlooked. Prior work by Addlagatta and coworkers[37] identified 20 C–H···S contacts with C···S distances up to 4 Å in enzyme-ligand binding sites reported in the PDB. Now, informed by the over 423,000 C–H···S contacts found in molecular structures of small molecules, we see that this 4 Å cut-off may be too short (Fig. S2e). We suspect lengthening the allowed range of C···S contact distances would reveal even more overlooked C–H···S hydrogen bonds present in enzyme-ligand binding sites in the PDB. In addition to our own analyses that establishes C–H···S close contacts as hydrogen bonds, we highlighted selected prior examples in which C–H···S contacts are present, but that were not identified in the earlier analyses. One such example from the hydrosulfide Hb complexes in *L. Pectinata* and human myoglobin may explain the disparate reactivity observed between the two Hb species.

As a whole, this review clearly highlights that C–H···S close contacts can be classified as HB interactions and should no longer be overlooked. The 3D histograms presented provide a convenient tool for identifying relatively strong, moderate, and weak C–H···S hydrogen bonds present in the solid state. Moving forward, we anticipate that the C–H···S interactions should be included in the design, analysis, and function of compounds in diverse areas of chemistry ranging from supramolecular chemistry to structural biology to materials characterization.

Conflicts of interest

There are no conflicts to declare.

Acknowledgements

We thank the Murdock Charitable Trust (201811528 to M.D.P./D.W.J.), the NIH (R01-GM087398 to D.W.J./M.M.H and F32-GM139372 to T.J.S.), and the NSF (CHE-2107602 to M.D.P.) for support of this research. This work was also supported by the Bradshaw and Holzapfel Research Professorship in Transformational Science and Mathematics to D.W.J.

References

1. L. C. Pauling, *The Nature of the Chemical Bond*, Cornell University Press, Ithaca, NY, 1st ed.,1939; 2nd ed., 1940, 3rd ed., 1960.
2. D. J. Liptrot and P. P. Power, *Nature Reviews Chemistry*, 2017, **1**, 0004.
3. E. A. Meyer, R. K. Castellano and F. Diederich, *Angew. Chem. Int. Ed.*, 2003, **42**, 1210-1250.
4. R. Paulini, K. Müller and F. Diederich, *Angew. Chem. Int. Ed.*, 2005, **44**, 1788-1805.
5. B. R. Beno, K.-S. Yeung, M. D. Bartberger, L. D. Pennington and N. A. Meanwell, *J. Med. Chem.*, 2015, **58**, 4383-4438.
6. E. Arunan, G. R. Desiraju, R. A. Klein, J. Sadlej, S. Scheiner, I. Alkorta, D. C. Clary, R. H. Crabtree, J. J. Dannenberg, P. Hobza, H. G. Kjaergaard, A. C. Legon, B. Mennucci and D. J. Nesbitt, *Pure Appl. Chem.*, 2011, **83**, 1619-1636.
7. E. Arunan, G. R. Desiraju, R. A. Klein, J. Sadlej, S. Scheiner, I. Alkorta, D. C. Clary, R. H. Crabtree, J. J. Dannenberg, P. Hobza, H. G. Kjaergaard, A. C. Legon, B. Mennucci and D. J. Nesbitt, *Pure Appl. Chem.*, 2011, **83**, 1637-1641.
8. G. R. Desiraju, *Angew. Chem. Int. Ed.*, 2011, **50**, 52-59.
9. J. E. Lennard-Jones, *Proc. Phys. Soc.*, 1931, **43**, 461-482.
10. D. June Sutor, *Nature*, 1962, **195**, 68-69.
11. J. Cai and J. L. Sessler, *Chem. Soc. Rev.*, 2014, **43**, 6198-6213.
12. Y. Li and A. H. Flood, *Angew. Chem. Int. Ed.*, 2008, **47**, 2649-2652.
13. Y. Liu, W. Zhao, C.-H. Chen and A. H. Flood, *Science*, 2019, **365**, 159-161.
14. L. M. Eytel, H. A. Fargher, M. M. Haley and D. W. Johnson, *Chemical Communications*, 2019, **55**, 5195-5206.
15. M. Lisbjerg, H. Valkenier, B. M. Jessen, H. Al-Kerdi, A. P. Davis and M. Pittelkow, *J. Am. Chem. Soc.*, 2015, **137**, 4948-4951.
16. S. Lee, C.-H. Chen and A. H. Flood, *Nature Chem.*, 2013, **5**, 704-710.
17. J. F. J. Dippy, *Chemical Reviews*, 1939, **25**, 151-211.
18. Y. Gu, T. Kar and S. Scheiner, *J. Am. Chem. Soc.*, 1999, **121**, 9411-9422.
19. E. B. Starikov and T. Steiner, *Acta Crystallogr. Sect. D.*, 1997, **53**, 345-347.
20. E. J. Corey, D. Barnes-Seeman and T. W. Lee, *Tetrahedron Lett.*, 1997, **38**, 1699-1702.
21. M. N. Grayson, Z. Yang and K. N. Houk, *J. Am. Chem. Soc.*, 2017, **139**, 7717-7720.
22. R. C. Johnston and P. H.-Y. Cheong, *Org. Biomolec. Chem.*, 2013, **11**, 5057-5064.

23. Y. Itoh, Y. Nakashima, S. Tsukamoto, T. Kurohara, M. Suzuki, Y. Sakae, M. Oda, Y. Okamoto and T. Suzuki, *Sci. Rep.*, 2019, **9**, 767.
24. B. W. Tresca, R. J. Hansen, C. V. Chau, B. P. Hay, L. N. Zakharov, M. M. Haley and D. W. Johnson, *J. Am. Chem. Soc.*, 2015, **137**, 14959-14967.
25. B. W. Tresca, A. C. Brueckner, M. M. Haley, P. H. Y. Cheong and D. W. Johnson, *J. Am. Chem. Soc.*, 2017, **139**, 3962-3965.
26. P. Zhou, F. Tian, F. Lv and Z. Shang, *Proteins*, 2009, **76**, 151-163.
27. V. R. Mundlapati, S. Ghosh, A. Bhattacherjee, P. Tiwari and H. S. Biswal, *J. Phys. Chem. Lett.*, 2015, **6**, 1385-1389.
28. L. A. H. van Bergen, M. Alonso, A. Palló, L. Nilsson, F. De Proft and J. Messens, *Sci. Rep.*, 2016, **6**, 30369.
29. M. Juanes, R. T. Saragi, R. Pinacho, J. E. Rubio and A. Lesarri, *Physical Chemistry Chemical Physics*, 2020, **22**, 12412-12421.
30. H. A. Fargher, N. Lau, H. C. Richardson, P. H.-Y. Cheong, M. M. Haley, M. D. Pluth and D. W. Johnson, *J. Am. Chem. Soc.*, 2020, **142**, 8243-8251.
31. M. D. Hartle, R. J. Hansen, B. W. Tresca, S. S. Prakel, L. N. Zakharov, M. M. Haley, M. D. Pluth and D. W. Johnson, *Angew. Chem. Int. Ed.*, 2016, **55**, 11480-11484.
32. N. Lau, L. N. Zakharov and M. D. Pluth, *Chemical Communications*, 2018, **54**, 2337-2340.
33. J. Vazquez and V. Sindelar, *Chemical Communications*, 2018, **54**, 5859-5862.
34. B. W. Tresca, L. N. Zakharov, C. N. Carroll, D. W. Johnson and M. M. Haley, *Chemical Communications*, 2013, **49**, 7240-7242.
35. T. J. Sherbow, L. N. Zakharov, D. W. Johnson and M. D. Pluth, *Inorg. Chem.*, 2020, **59**, 15574-15578.
36. S. Ghosh, P. Chopra and S. Wategaonkar, *Physical Chemistry Chemical Physics*, 2020, **22**, 17482-17493.
37. R. Reddi, K. K. Singarapu, D. Pal and A. Addlagatta, *Mol. Biosyst.*, 2016, **12**, 2408-2416.
38. M. McDougall, O. Francisco, C. Harder-Viddal, R. Roshko, M. Meier and J. Stetefeld, *Proteins*, 2017, **85**, 2209-2216.
39. J. Hwang, P. Li, M. D. Smith, C. E. Warden, D. A. Sirianni, E. C. Vik, J. M. Maier, C. J. Yehl, C. D. Sherrill and K. D. Shimizu, *J. Am. Chem. Soc.*, 2018, **140**, 13301-13307.
40. We did consider crystal structure quality when analyzing the CSD data, and this information can be found in the "Assessing the importance of crystal structure quality" section in the Supporting Information.
41. P. Mondal, E. Solel, N. Fridman, E. Keinan and O. Reany, *Chem. Eur. J.*, 2019, **25**, 13336-13343.
42. M. M. Cerda, T. D. Newton, Y. Zhao, B. K. Collins, C. H. Hendon and M. D. Pluth, *Chem. Sci.*, 2019, **10**, 1773-1779. PMCID: PMC6368244.
43. T. Steiner, *Angew. Chem. Int. Ed.*, 2002, **41**, 48-76.
44. J. Kroon and J. A. Kanters, *Nature*, 1974, **248**, 667-669.
45. A. Bondi, *J. Phys. Chem.*, 1964, **68**, 441-451.
46. T. Steiner and G. R. Desiraju, *Chemical Communications*, 1998, 891-892.
47. J.-A. van den Berg and K. R. Seddon, *Cryst. Growth Des.*, 2003, **3**, 643-661.
48. A. Sengupta, Y. Liu, A. H. Flood and K. Raghavachari, *Chem. Eur. J.*, 2018, **24**, 14409-14417.
49. G. A. Jeffrey, *An Introduction to Hydrogen Bonding*, Oxford University Press, 1997.
50. J. S. Laursen, J. Engel-Andreasen, P. Fristrup, P. Harris and C. A. Olsen, *J. Am. Chem. Soc.*, 2013, **135**, 2835-2844.
51. A. Raghuvanshi, A. K. Jha, A. Sharma, S. Umar, S. Mishra, R. Kant and A. Goel, *Chem. Eur. J.*, 2017, **23**, 4527-4531.
52. L. Viglianti, N. L. C. Leung, N. Xie, X. Gu, H. H. Y. Sung, Q. Miao, I. D. Williams, E. Licandro and B. Z. Tang, *Chem. Sci.*, 2017, **8**, 2629-2639.
53. M. Ghosh, P. Panwaria, S. Tothadi, A. Das and S. Khan, *Inorg. Chem.*, 2020, **59**, 17811-17821.
54. T. Steiner, *J. Mol. Struct.*, 1998, **447**, 39-42.
55. N. Lau and M. D. Pluth, *Curr. Opin. Chem. Biol.*, 2019, **49**, 1-8.
56. I. Hisaki, Y. Sakamoto, H. Shigemitsu, N. Tohnai, M. Miyata, S. Seki, A. Saeki and S. Tagawa, *Chem. Eur. J.*, 2008, **14**, 4178-4187.
57. C. Roche, Q. Luo, G. Gil-Ramírez, H.-W. Jiang, D. R. Kohn, Y. Xiong, A. L. Thompson and H. L. Anderson, *J. Org. Chem.*, 2017, **82**, 7446-7462.
58. B. K. Czyzewski and D.-N. Wang, *Nature*, 2012, **483**, 494-497.
59. Due to the similar size between Cl^- and HS^- the authors who published PDB: 3TDX note that protein crystallography would have difficulty distinguishing between the two anions, however this structure was grown from a HS^- solution and so they believe that HS^- is in the ion channel.
60. S.-J. Chiou, C. G. Riordan and A. L. Rheingold, *Proc. Natl. Acad. Sci. USA*, 2003, **100**, 3695-3700.
61. C. D. Sessler, M. Rahm, S. Becker, J. M. Goldberg, F. Wang and S. J. Lippard, *J. Am. Chem. Soc.*, 2017, **139**, 9325-9332.
62. J. P. Shanahan, D. M. Mullis, M. Zeller and N. K. Szymczak, *J. Am. Chem. Soc.*, 2020, **142**, 8809-8817.
63. The overwhelming majority of sulfur based ligands have sulfur in the -2 oxidation state. The only exception is bound polysulfides which make up 2.3% of the total molecules in the search.
64. S. S. Batsanov, *Inorg. Mater.*, 2001, **37**, 871-885.
65. M. M. Cerda, Y. Zhao and M. D. Pluth, *J. Am. Chem. Soc.*, 2018, **140**, 12574-12579. PMCID: PMC6504978.
66. R. Wang, *Physiol. Rev.*, 2012, **92**, 791-896.
67. V. Vitvitsky, P. K. Yadav, A. Kurthen and R. Banerjee, *J. Biol. Chem.*, 2015, **290**, 8310-8320.
68. T. Bostelaar, V. Vitvitsky, J. Kumutima, B. E. Lewis, P. K. Yadav, T. C. Brunold, M. Filipovic, N. Lehnert, T. L. Stemmler and R. Banerjee, *J. Am. Chem. Soc.*, 2016, **138**, 8476-8488.
69. V. Vitvitsky, P. K. Yadav, S. An, J. Seravalli, U.-S. Cho and R. Banerjee, *J. Biol. Chem.*, 2017, **292**, 5584-5592.
70. M. R. Filipovic, J. Zivanovic, B. Alvarez and R. Banerjee, *Chemical Reviews*, 2018, **118**, 1253-1337.
71. M. Rizzi, J. B. Wittenberg, A. Coda, P. Ascenzi and M. Bolognesi, *J. Mol. Biol.*, 1996, **258**, 1-5.
72. V. Vitvitsky, P. K. Yadav, S. An, J. Seravalli, U.-S. Cho and R. Banerjee, *J. Biol. Chem.*, 2017, **292**, 5584-5592.
73. R. Pietri, A. Lewis, R. G. León, G. Casabona, L. Kiger, S.-R. Yeh, S. Fernandez-Alberti, M. C. Marden, C. L. Cadilla and J. López-Garriga, *Biochemistry*, 2009, **48**, 4881-4894.
74. E. Galardon, A. Tomas, M. Selkti, P. Roussel and I. Artaud, *Inorg. Chem.*, 2009, **48**, 5921-5927.
75. E. Galardon, A. Tomas, P. Roussel and I. Artaud, *Eur. J. Inorg. Chem.*, 2011, **2011**, 3797-3801.

Author Profiles:

Hazel A. Fargher earned her BS in chemistry from Worcester Polytechnic Institute in 2016, where she performed research with Prof. Marion H. Emmert. From there, she earned her PhD in chemistry at the University of Oregon under the guidance of Profs. Darren W. Johnson and Michael M. Haley. Her thesis work was on a collaborative project with the Prof. Michael D. Pluth group, using physical organic techniques to study host-guest chemistry of the hydrochalcogenide anions.

Tobias J. Sherbow earned his BS in chemistry from the University of Oregon in 2012, performing undergraduate research with Prof. David Tyler. He earned his PhD in 2019 from UC Davis studying proton and electron transfer reactions of group 13 complexes with Prof. Louise Berben. Toby is now an NIH NRSA fellow at the University of Oregon under the joint direction of Profs. Michael Pluth and Darren Johnson studying the molecular recognition and reactivity of reactive sulfur species.

Michael M. Haley received his BA (1987) and PhD (1991) degrees from Rice University in Houston, Texas. After a postdoctoral stay at the University of California, Berkeley, he joined the faculty at the University of Oregon in 1993 where he currently is the Richard M. and Patricia H. Noyes Professor of Chemistry. He also served as Head of the Department from 2008 to 2014. Haley has co-authored over 230 research articles and is co-inventor on 13pending and issued patents. His current research interests focus on the synthesis and properties of antiaromatic organic semiconductors and on phenylacetylene-based molecular scaffolds for anion sensing.

Darren W. Johnson is the Bradshaw and Holzapfel Research Professor in Transformational Science and Mathematics at the University of Oregon and a Professor of Chemistry. He performed undergraduate research with Jonathan Sessler at UT-Austin, where he earned his B.Sc. in Chemistry in 1996. He obtained his Ph.D. in Ken Raymond's lab at UC-Berkeley in 2000 and was an NIH NRSA post-doctoral researcher at the Scripps Research Institute with Julius Rebek, Jr. from 2001-2003. He has been at the University of Oregon since 2003, where research in the group uses supramolecular chemistry as a tool to explore a variety of problems in self-assembly, molecule/ion recognition, and inorganic cluster synthesis.

Michael D. Pluth earned his BS in chemistry and applied mathematics from the University of Oregon in 2004, conducting undergraduate research with Prof. David Tyler. He earned his PhD in 2008 from UC Berkeley as an NSF predoctoral fellow under the joint direction of Profs. Robert Bergman and Kenneth Raymond. Mike then moved to MIT as an NIH NRSA and later NIH Pathway to Independence Postdoctoral Fellow with Prof. Stephen Lippard. Mike began his independent career at the University of Oregon in 2011. His research interests are thematically based on different aspects of chemical biology and physical organic chemistry of reactive sulfur species.

TOC Image:

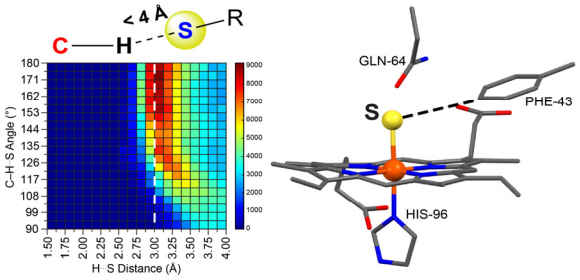

Characterizing C–H···S hydrogen bonding interactions